[AMERICAN JOURNAL OF SCIENCE, VOL. 291, MARCH, 1991, P. 284–308]

PHANEROZOIC PALEOGEOLOGY

GREGG J. S. BLUTH* and LEE R. KUMP
Department of Geosciences and Earth System Science Center, The Pennsylvania State University, University Park, Pennsylvania 16802

ABSTRACT. Current geochemical cycling models do not account for changes in the spatial distribution of rock exposed to weathering through time. As a step in this direction, a new method of constructing paleogeologic maps has been developed, using published, global, depositional lithofacies maps. This technique identifies areas of erosion for a given interval of time, then systematically searches back through lithofacies maps of progressively older periods to determine the most probable type of rock being weathered during the interval. The age-area results for present-day sedimentary exposures show the same lognormal relationship previously determined by Blatt and Jones (1975). A geologic map of the Recent generated by this method reproduces the general igneous, marine, and continental clastic spatial and temporal distributions found in current outcrops. However, the total exposure area of sandstones is larger than previous estimates based on volume, not areal proportions. We propose that exposed sandstone deposits are extensive, but thin (and thus represent a much smaller volume than areal proportion of sedimentary rocks).

The relative proportions of exposed rock types through Phanerozoic time show few abrupt changes compared to the secular changes in the areal extent of the depositional lithologies. The global distribution of exposed rock types through time suggests that exposed cratonic shield areas have generally been replaced in extent with clastic sediments, but this trend may be an artifact of the mapping technique. For paleoclimate modeling, these determinations of paleogeologic distribution should ultimately provide a great advantage over parameterizations based on global estimates of sedimentary reservoirs.

INTRODUCTION

Models of global geochemical cycles of the elements generally lack a spatial dimension and have not been designed to take advantage of a growing knowledge of paleogeography. For example, in the widely cited BLAG model (Berner, Lasaga, and Garrels, 1983) and in subsequent versions (Lasaga, Berner, and Garrels, 1985; Berner, 1990), an average climate (runoff and temperature) is determined for a given time step in the model run using greenhouse/climate relationships. Empirical formulas that relate climate, runoff, and river composition are then used to calculate global fluxes of major dissolved cations and anions. However, there is no allowance for spatial heterogeneity of climate or geologic exposure in this zero–spatial–dimension model.

A first step in adding a spatial dimension to such models is to determine the paleogeology, that is, the geographic distribution of the types of rocks undergoing weathering during a given period of time.

* Present address: NASA Goddard Space Flight Center, Code 921, Greenbelt, Maryland 20771

Previous work in this area has been rather limited. Levorsen (1960) set out the proper procedures for the determination of paleogeology based on geologic maps of the present world, outcrop and core information, and stratigraphic principles. Cook and Bally (1975) utilized these procedures to develop a set of maps of strata underlying Paleozoic sedimentary rocks in North and Central America. The sedimentary strata, however, were identified only by age, so their utility in constructing paleogeologies for geochemical cycling models was rather limited.

Here we describe a method of reconstructing exposures of Phanerozoic rock types from maps of volcanic and sediment deposition. The ultimate objectives are to assess (1) the possibility that the abundance and geographic distribution of geologic exposures differed significantly in the past, and (2) the potential effect these differences might have had on atmospheric CO_2 and global climate. Our aim here is to produce paleogeologic maps that define the type of rock being weathered at a given time and place with a much higher degree of accuracy than by a global average rock type. Expected age-area relationships and replication of present-day exposures appear in the paleogeologic results, suggesting that they indeed capture the general nature of change in the types of rock being weathered over Phanerozoic time.

PALEOGEOLOGIC MAP CONSTRUCTION

We have developed a general procedure for determining the spatial and temporal distribution of exposed geologic units from the series of paleolithofacies maps generated by A.B. Ronov and his colleagues over the last few decades. These maps present the presumed original extent of deposition, which was determined by Ronov's group based on preserved distributions. The following steps are used for each time period of interest:

1. Ronov's maps are first divided into 2 degree longitude by 2 degree latitude grids (present geography). The information on volcanic and sedimentary deposition during a given time period is then digitized from the lithofacies maps. Each grid is either assigned a rock type value or is designated as an area of erosion or no record (typically regions overlying oceanic crust). The data are then entered into the computer as a 180×90 matrix for processing (fig. 1A).

2. To create a paleogeologic map, any grids representing regions of contemporaneous sediment deposition or igneous activity on land are assumed to have been exposed to weathering processes at some time during the period and are included in the geologic map of the period. Grids representing regions of erosion (presumed land) are then identified; these same grids on earlier maps are successively inspected until either a depositional rock designation is encountered or the oldest map is reached (fig. 1B and C). This designation is then used to represent the type of rock that was most likely being weathered during the time period.

3. Areas for which no rock types are found are temporarily labeled "untyped." An untyped region is assumed to represent cratonic shield area older than Early Proterozoic.

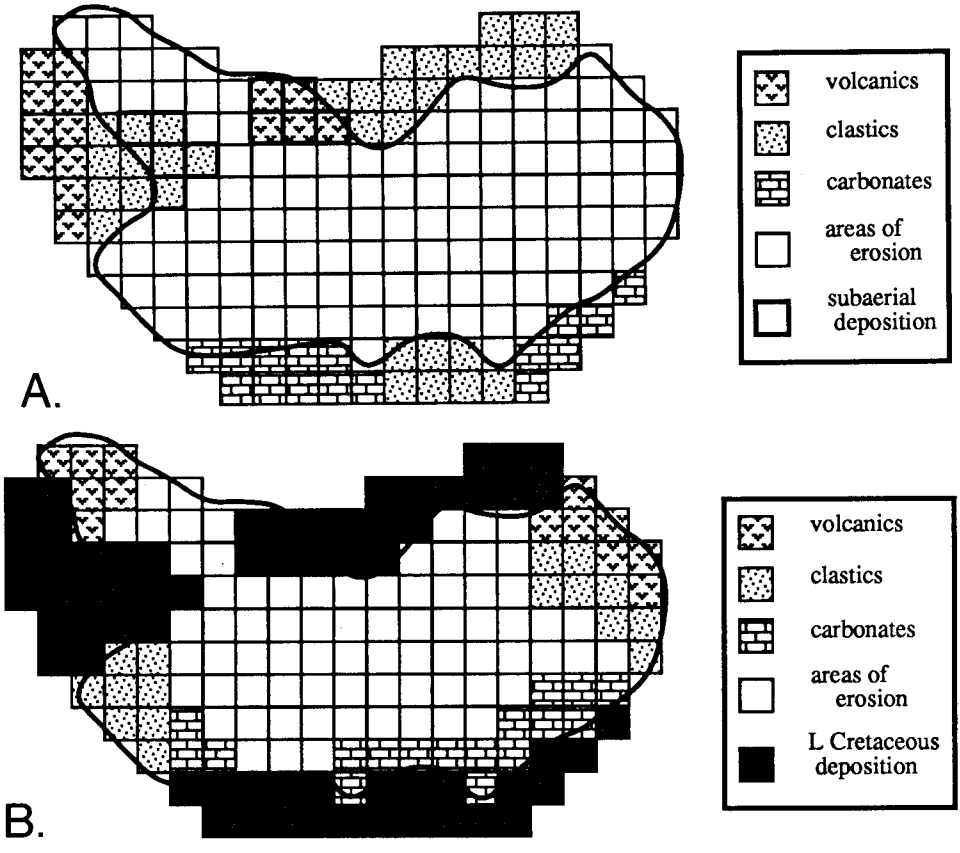

Fig. 1. Construction of "Late Cretaceous" geologic map. (A) "Late Cretaceous" lithofacies map and outline of an idealized continent. (B) Areas of "Late Cretaceous" erosion underlain by "Early Cretaceous" deposits are identified.

The culmination of this process is the paleogeologic map (fig. 1D). (For clarity, fig. 1 ignores any pre-"Late Jurassic" contributions to "Late Cretaceous" paleogeology.) It includes areas undergoing penecontemporaneous, subaerial deposition as well as areas of subaerial exposure. The map remains in a present-day, geographic orientation. In the future we will rotate all maps into their paleogeographic configurations, to study the Phanerozoic climate/weathering connection.

PALEOGEOLOGIC MAPS OF THE PHANEROZOIC

The primary data base of paleolithofacies maps prepared by Ronov and his colleagues is listed in table 1. The most detailed and up-to-date

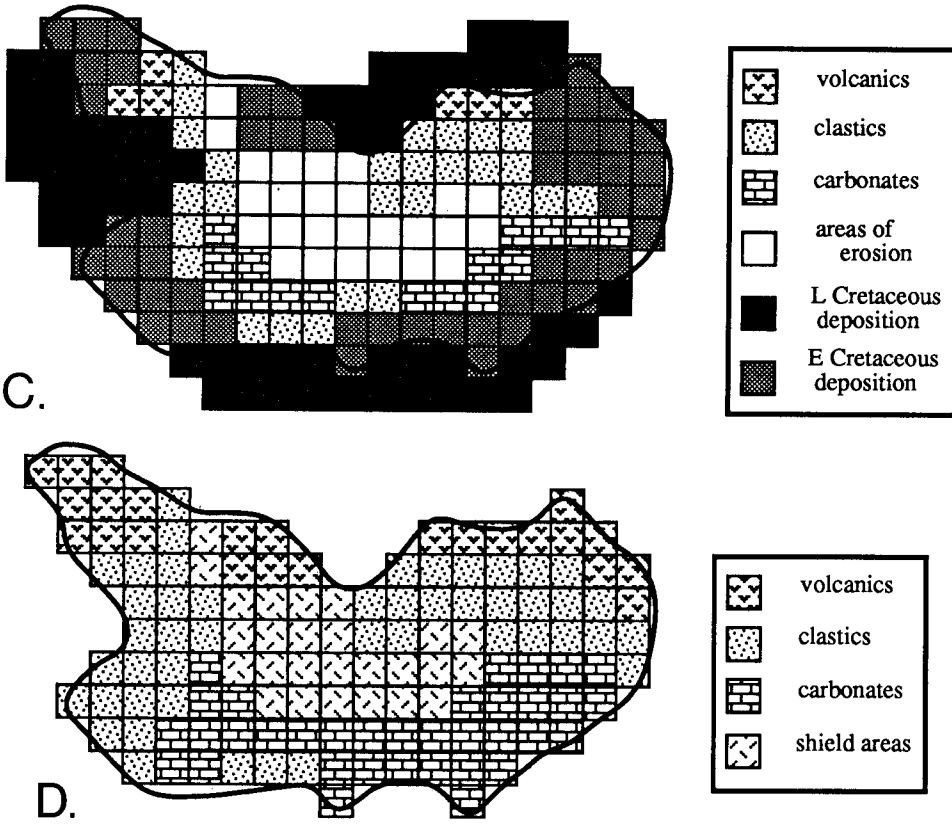

(C) Remaining areas of erosion underlain by "Late Jurassic" deposits are identified. (D) Final, reconstructed geologic map for the "Late Cretaceous." Areas of erosion in "Late Cretaceous" for which no earlier deposits were found (neglecting, for simplicity, pre-"Late Jurassic" deposits) designated as shield (crystalline basement).

maps are those of the Paleozoic atlas (Ronov, Khain, and Seslavinskiy, 1984), while the Mesozoic and Cenozoic periods are covered in a series of individual papers published since the 1960's. Because the spectrum of designated rock types differs among these maps, we have consolidated Ronov's lithologic divisions into eight major groups: carbonate, evaporite, sandstone (terrigenous:sandy of Ronov), shale (terrigenous:sandy/argillaceous and clay of Ronov), coal-bearing shale, siliceous rock (chert), volcanic, and area of erosion.

The youngest geologic period represented in the database is the Pliocene. A modern-day geologic map has been derived, however, that differs from that of the Pliocene, because it includes regions of Pliocene subaqueous deposition that are now exposed. This map is subsequently

TABLE 1

Data sources for paleolithologic maps

Time Period	Reference
Pliocene, Miocene	Khain, Ronov, and Balukhovskiy (1979)
Oligocene, Eocene, Paleocene	Ronov, Khain, and Balukhovskiy (1978)
Late, Early Cretaceous	Khain, Ronov, and Balukhovskiy (1975)
Late Jurassic	Ronov, Khain, and Balukhovskiy (1983)
Middle, Early Jurassic	Ronov and Khain (1962)
Late, Middle, Early Triassic	Ronov and Khain (1961)
Late Permian to Early Riphean	Ronov, Khain, and Seslavinskiy (1984)

referred to as the "Recent;" bear in mind, however, that Quaternary exposures are not represented.

This method of geologic reconstruction presents some difficulty in dealing with untyped areas. Ideally, they represent exposures of pre-Riphean rocks: essentially the granites and gneisses of the continental cratons. In practice, areas for which the record of Phanerozoic deposition is completely lost are also included. In addition, one cannot determine from Ronov's data when the shields were first exposed; for some regions the maps show them as uncovered since the early Proterozoic. This assumption is later examined using the results from the geologic map of the Recent.

Our approach contains some other obvious weaknesses. First of all, it depends entirely on the accuracy of the lithofacies maps in terms of both the preserved distribution of sedimentary and igneous rocks and the inferred original extent of deposition. Secondly, the approach requires the determination of a single rock type for an area of 2 degree longitude by 2 degree latitude extent. One cell represents an area of approx 50,000 km^2 at the equator. In folded mountain belts a significant amount of important information on paleoweathering environments therefore could be lost. However, Ronov and his coworkers partially restored some folded regions during their compilations (Ronov and others, 1980). Third, the method cannot recognize the complete erosion of a given rock unit, much less the timing of when the underlying layer was exposed. For example, the results for the Recent show much of the Canadian shield as covered by sediments, because Ronov's group has attempted to represent the original extent of Paleozoic sediment deposition. Thus, sedimentary rock exposures are probably overrepresented, and continental shield exposures are underrepresented. Finally, some of the most significant environments in terms of global cycling (tectonically active areas, oceanic islands, smaller regions of limestone, or evaporite weathering) may be missing, either because of their small size or because of the low likelihood of their being preserved in the rock record.

Because of these limitations, it is unlikely that the maps discussed here fully reproduce past weathering lithologies. We will now assess the accuracy of these maps by looking at (1) the relationships between age

and exposed surface area, (2) the geology of the Recent map compared to present day exposures, and (3) the resultant trends over Phanerozoic time in the types of rocks being weathered.

AGE-AREA RELATIONSHIPS

Of the many assumptions built into geochemical cycling models, perhaps the most fundamental is that the flux of erosion products from a given rock type is proportional to its global reservoir mass. This assumption, however, would be true only if all rock types had (1) identical exposure-area/reservoir-mass ratios, and (2) uniform geographical distributions. Given the dependence of area/mass ratios on depositional environment (platform versus geosyncline), the geographical limits to the deposition of certain rock types (carbonates or evaporites), and the effects of plate motions, there is reason to suspect the validity of this assumption.

The connection between surface area of exposure and mass of a sedimentary reservoir is assumed because of the observation of similar relationships between both the mass and the area of exposure of sedimentary rocks and their age. This relationship, which is lognormal, was first discovered in sedimentary mass-age data by Gregor (1968). Garrels and Mackenzie (1971) argued that the mass-age distribution is consistent with a model in which the total rate of sediment recycling has been invariant in time, and the erosion rate for rock of a specific age is proportional to its total mass.

Of course, weathering rates are at best proportional to the exposure area of rocks of a given age or type. Blatt and Jones (1975) determined the area of exposure of sedimentary rocks as a function of their age and also found a lognormal distribution that yields a half-age of sedimentary rocks of 130 my. This is similar to the half-age determined for mass-age distributions (140 my, Garrels and Mackenzie, 1971). There is a close similarity (fig. 2) between the updated mass distribution of Gregor (1985) and the areal distribution of sediments from Blatt and Jones (1975). The departure of both curves from ideal lognormal relationships illustrates how the sedimentary recycling rate has varied over geologic time.

The accuracy of the paleogeologic maps can be tested by investigating their age-area relationships. A close correspondence is found between our results and those of Blatt and Jones (1975) for the present day outcrop area of sediment (excluding Quaternary deposits), suggesting that the paleogeologic maps are capturing first order characteristics (fig. 3). Our results differ significantly from those of Blatt and Jones (1975) only in that we have a much larger contribution from the Tertiary. This difference is reconciled by the slightly smaller proportions from each successively older period.

We also observe that both curves are "bimodal" in nature, with significantly higher inferred recycling rates from 140 my to the present and prior to 350 my. The steeper slopes coincide with two major periods of continental collision and orogeny, times that should exhibit faster recycling rates of sediments (Mackenzie and Pigott, 1981; Worsley,

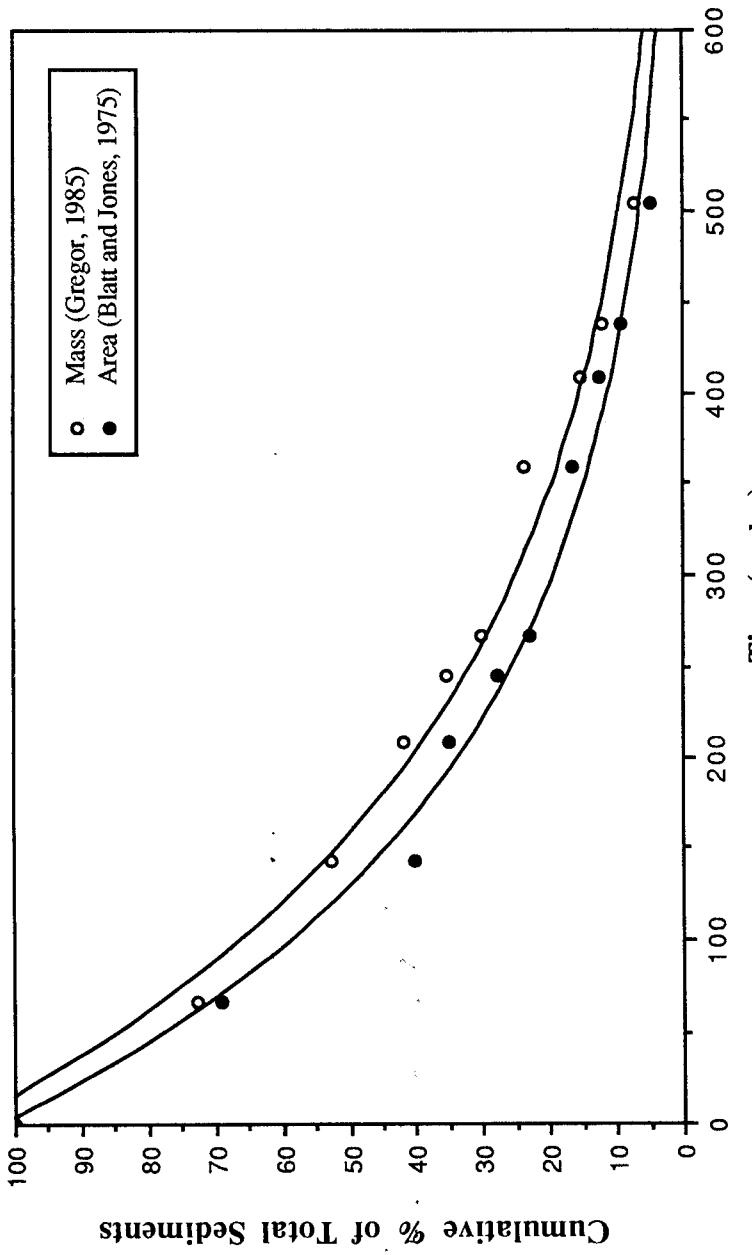

Fig. 2. Mass-age and exposure area-age relationships for Phanerozoic sediments.

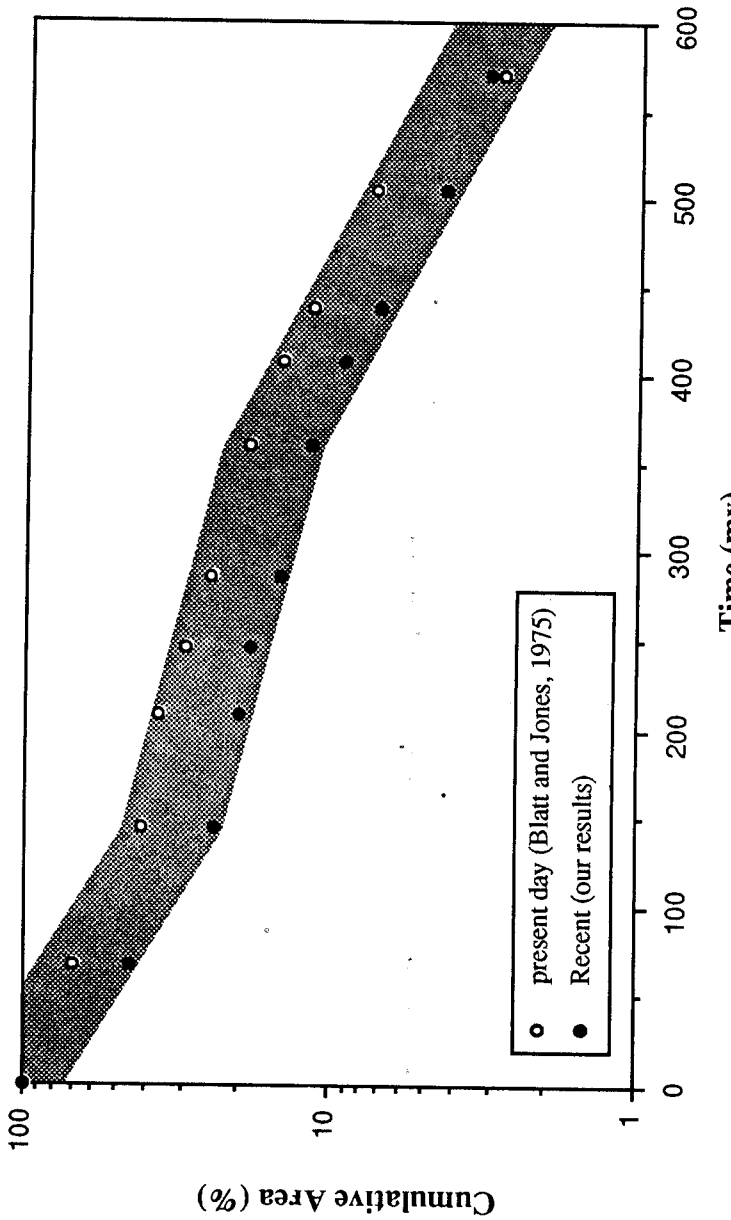

Fig. 3. Exposure area-age relationships from Blatt and Jones (1975) and from present work. The shaded area highlights two breaks in slope at the beginning of Cretaceous and Devonian time.

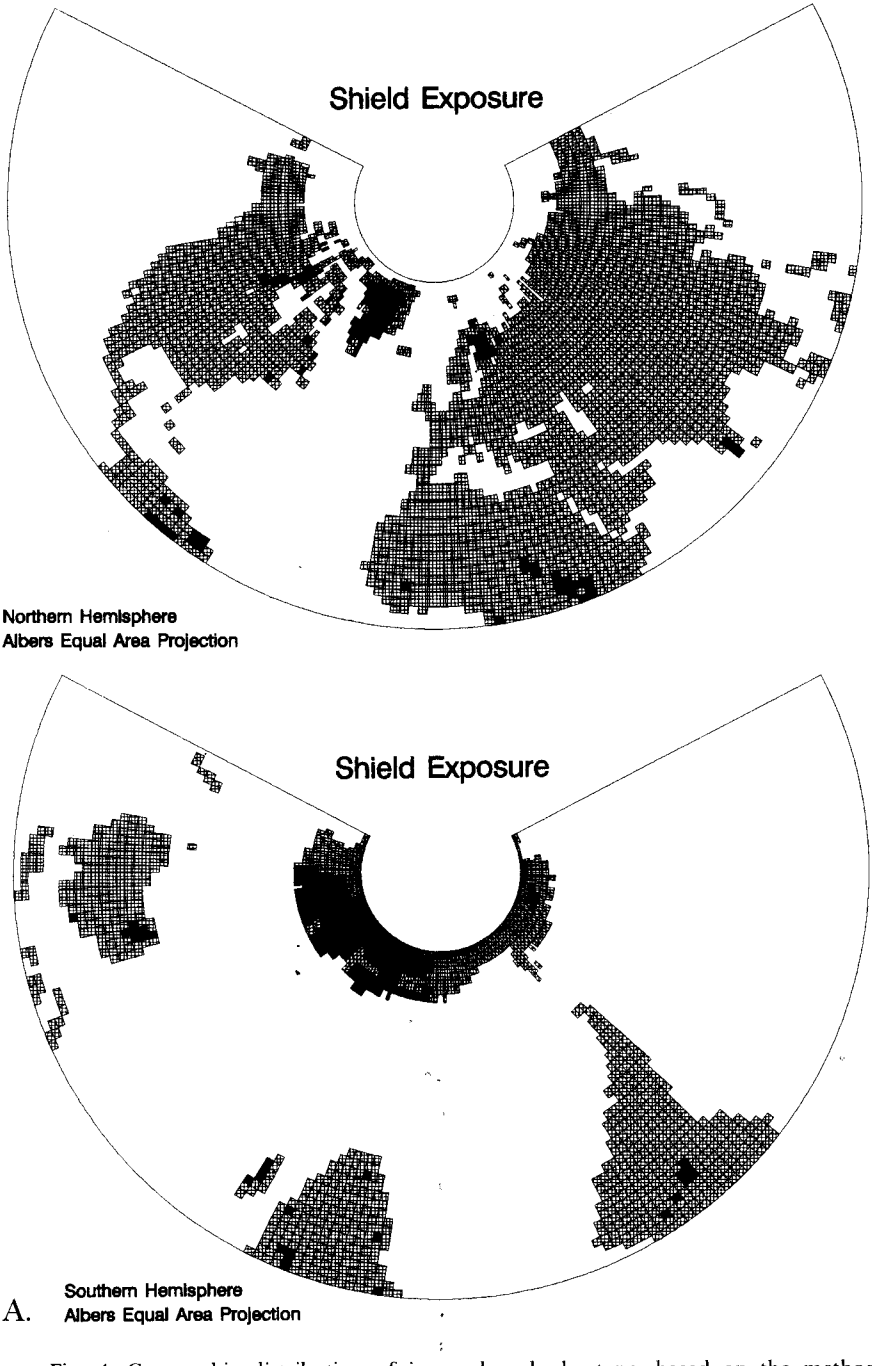

A.

Fig. 4. Geographic distribution of exposed rocks by type, based on the method described here. (A) Shield (crystalline basement).

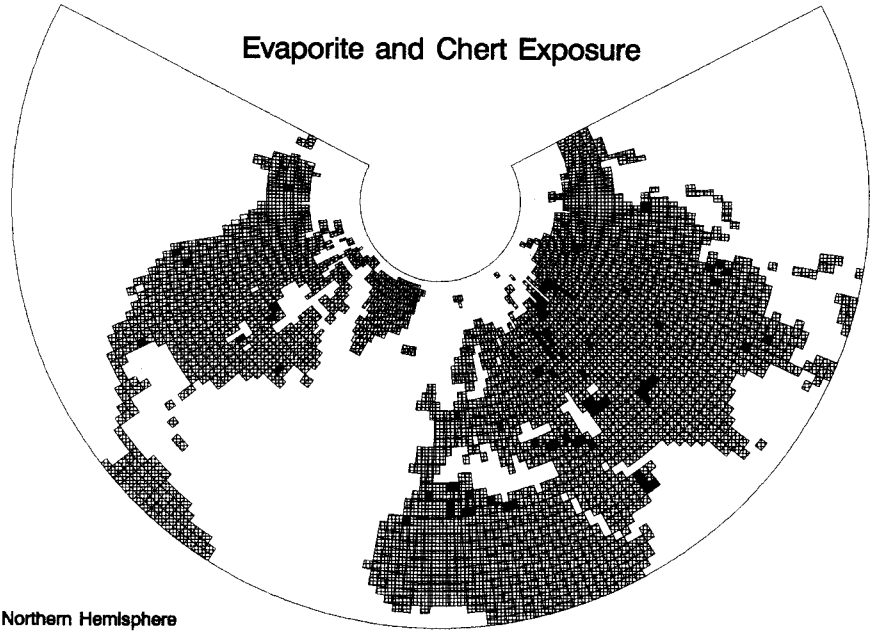

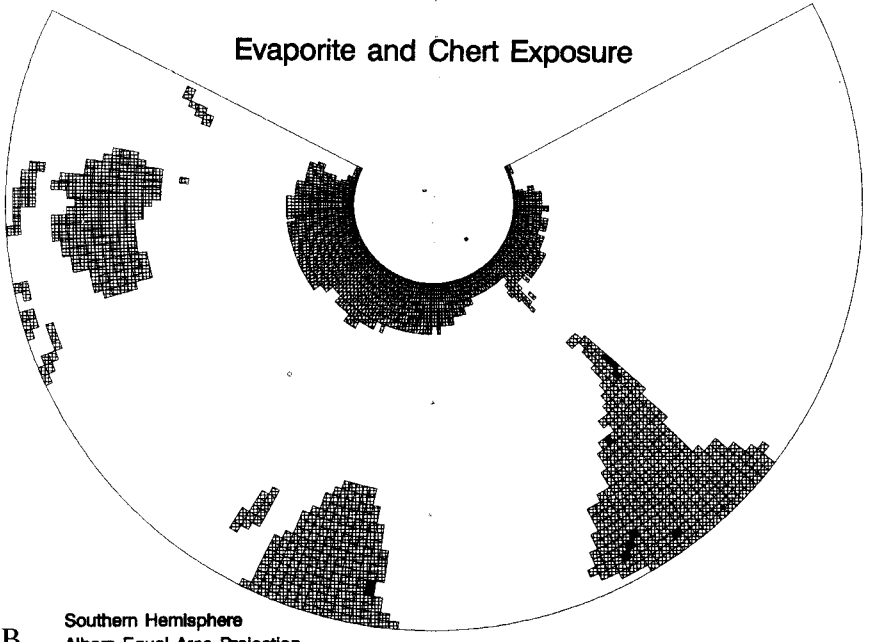

B.

(B) Evaporite and chert.

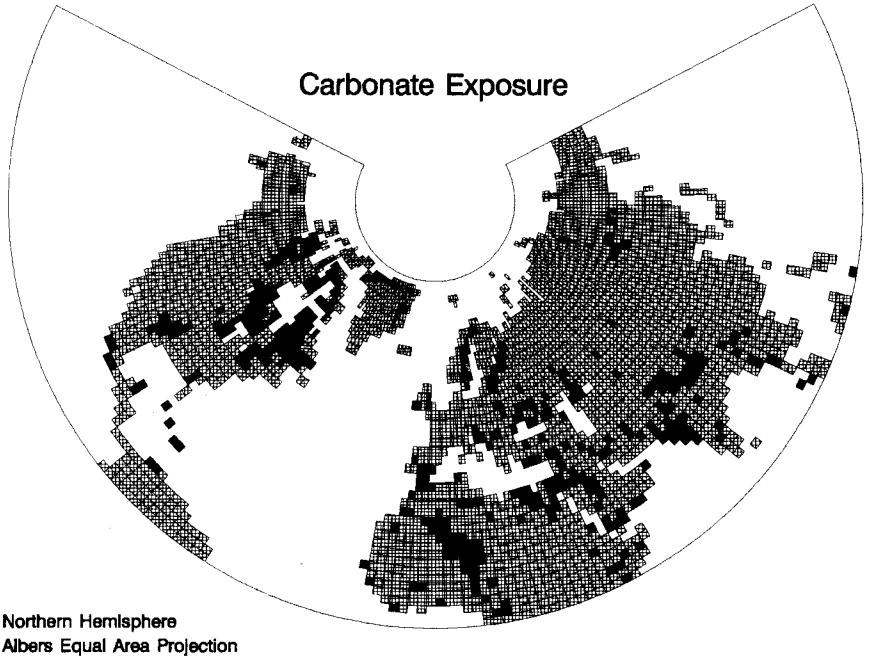

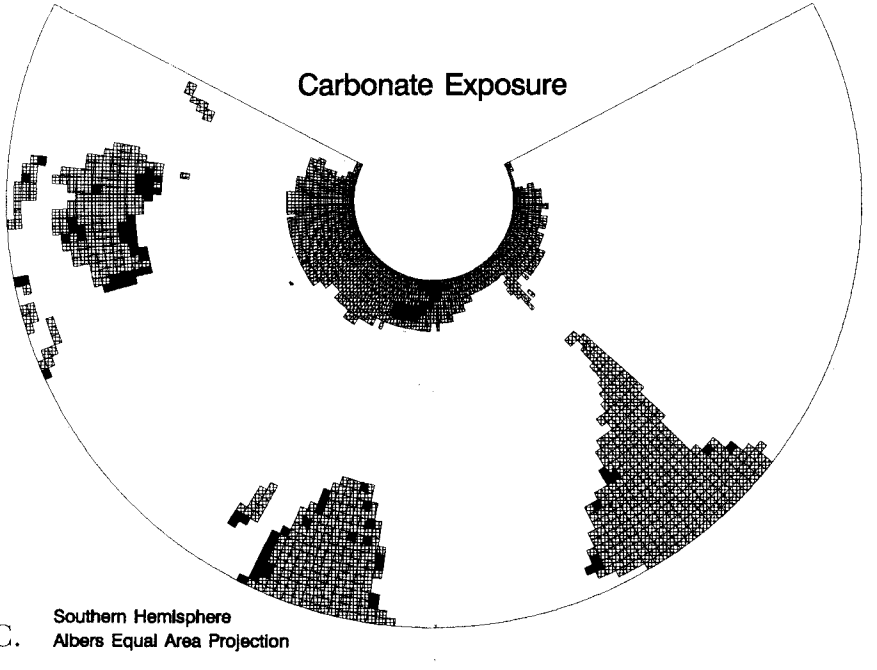

C.

Fig. 4 (continued) (C) Carbonate.

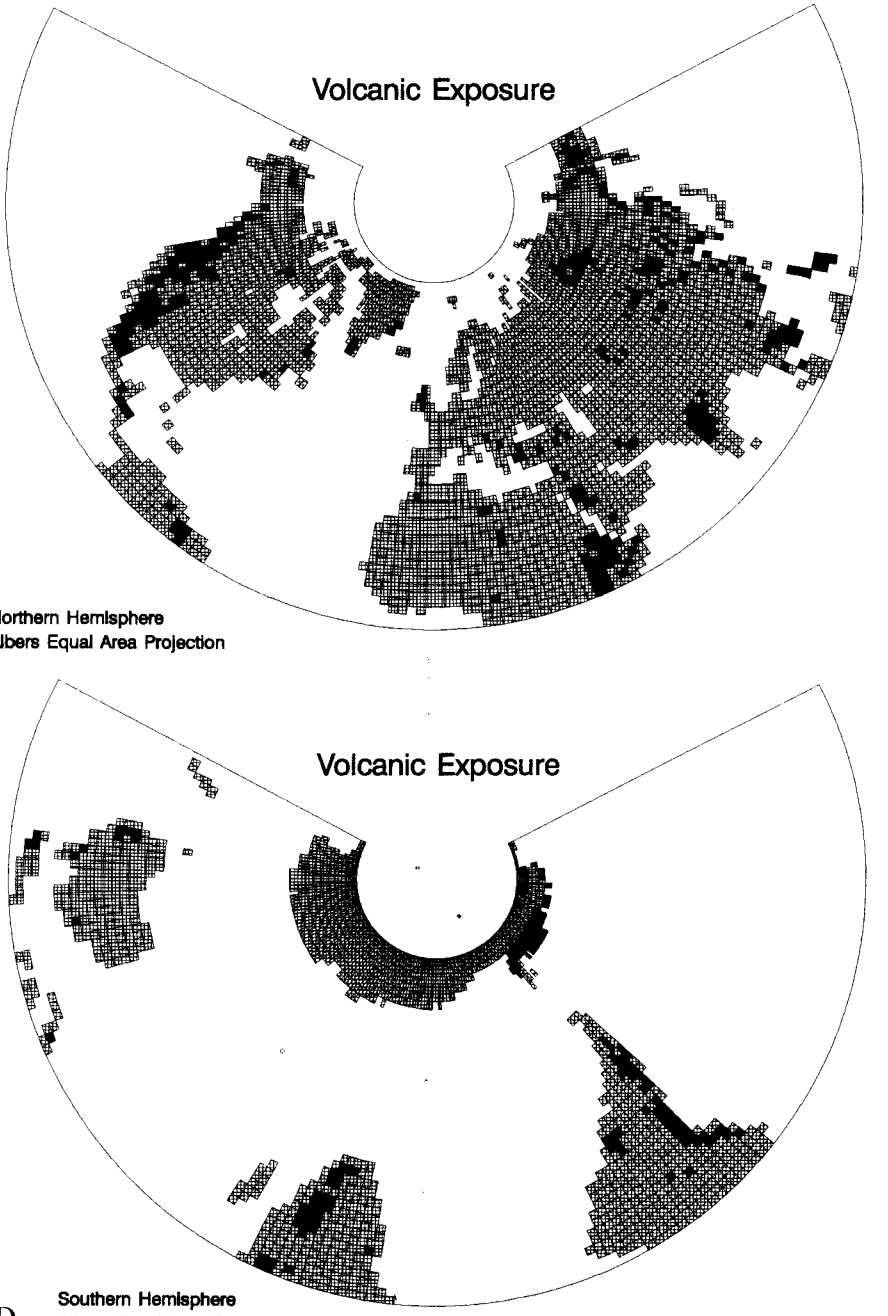

D.

(D) Volcanic rock.

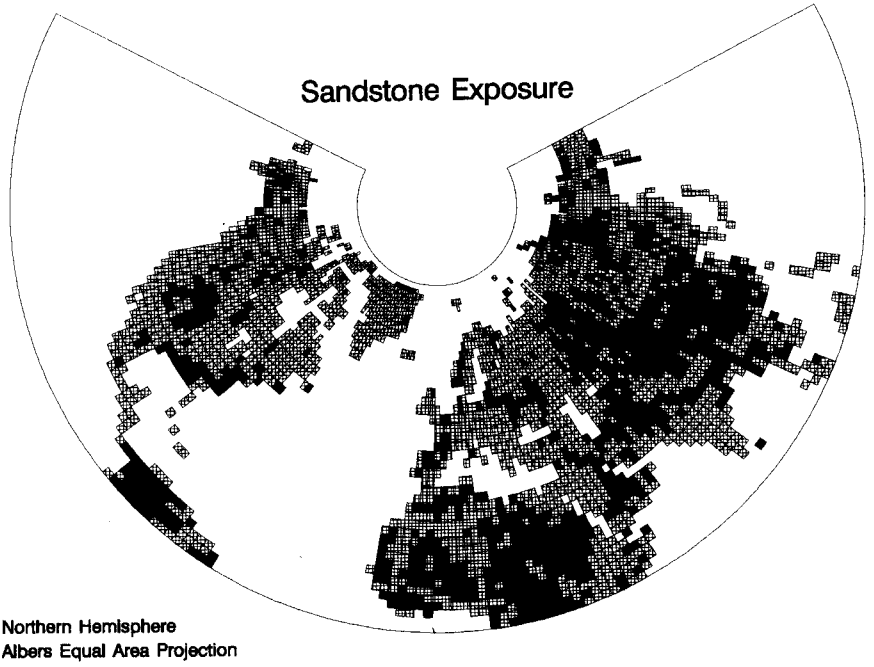

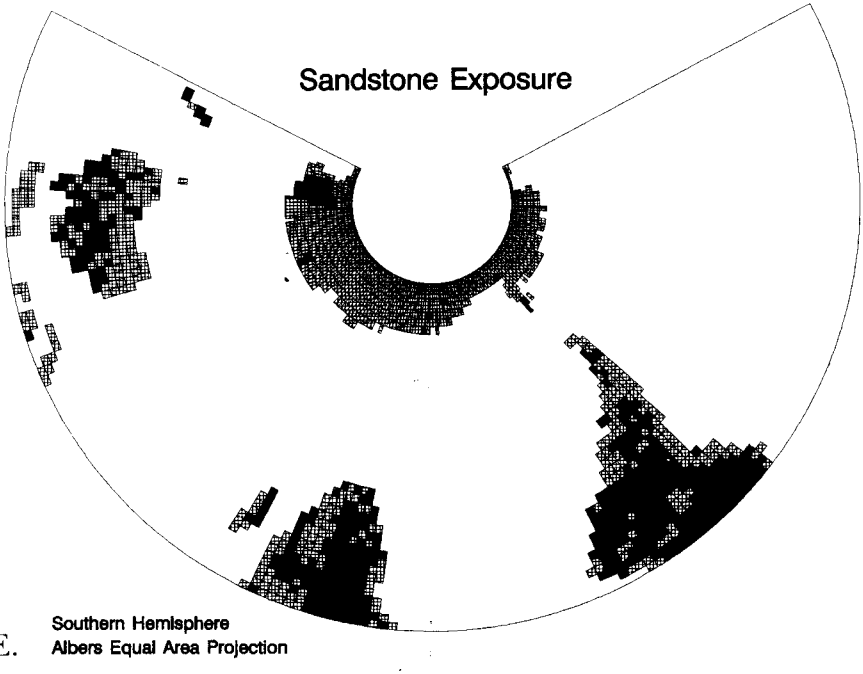

E.

Fig. 4 (continued) (E) Sandstone.

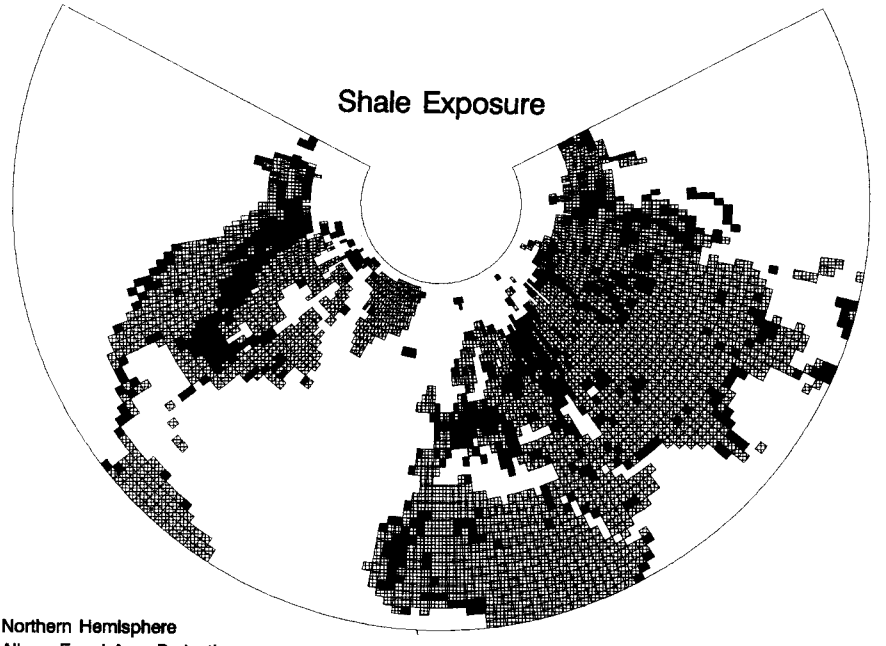

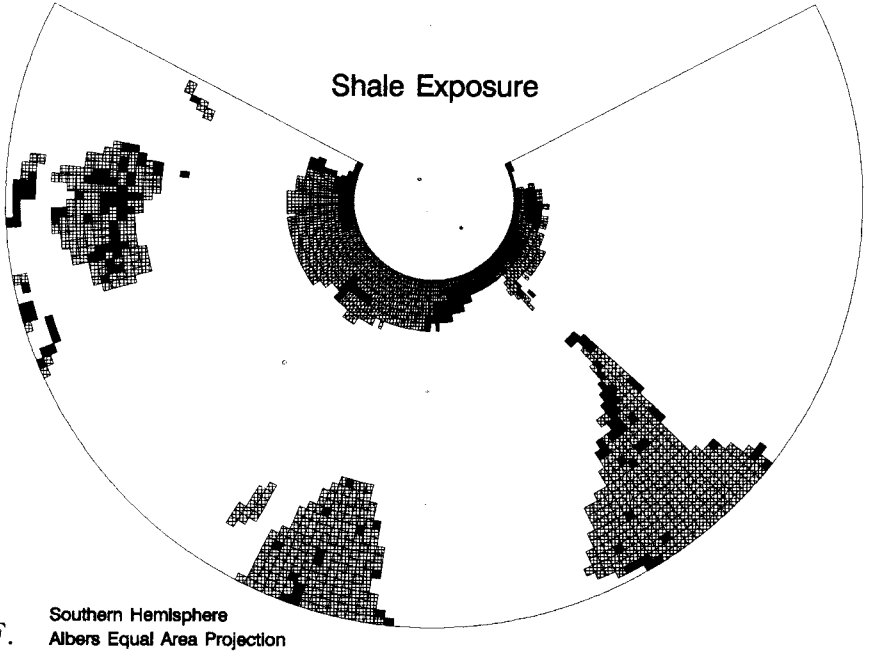

F.

(F) Shale. Exposure of Quaternary sediment is not included.

Nance, and Moody, 1986). Between these periods, continents were agglomerated into the supercontinent Pangea. Pangea may have weathered slowly because of aridity in its interior (Kutzbach and Gallimore, 1989). This, together with slower global rates of vertical tectonics, could explain the apparently slow recycling rates of the Late Paleozoic-Early Mesozoic.

GEOLOGIC FEATURES OF THE RECENT

The maps generated for the Recent (fig. 4) reproduce general features (excluding Quaternary deposits) of today's distribution of rocks exposed to weathering. Overall, the locations of continental shield exposure are correct (compare fig. 4A; Snead, 1980), but the areal extent of the shields is too small. Global distributions of economic quantities of coal, salt domes, potash, and phosphates compiled by Derry (1980) compare favorably with predicted areal extents of coal-bearing shales and evaporites (fig. 4B). Areas of carbonate exposure (fig. 4C), except where previously noted, are similar to present-day limestone and karst regions (Herak and Stringfield, 1972; Snead, 1980). Observed volcanic rock outcrops of the present-day (Choubert and Faure-Muret, 1981) are generally reproduced by the paleogeologic reconstructions (fig. 4D). Global exposures of clastic sediments (sandstone, fig. 4E; shale, fig. 4F) were verified on the basis of their ages, because both world-wide compilations (Cook and Bally, 1975; Choubert and Faure-Muret, 1981) identify sedimentary rocks by age rather than by lithology.

To demonstrate geographic variability in rock exposure, we have compiled the relative and absolute latitudinal distributions of rock types from the Recent map results (fig. 5; table 2). Present-day exposures on the large land masses of Africa and South America at low latitudes, North America and Eurasia at middle and high northern latitudes, and Antarctica at high southern latitudes, largely determine the latitudinal patterns. For example, deposition of sandstones has dominated sedimentation on Africa and South America throughout the Mesozoic and Cenozoic (Ronov, Khain, and Balukhovskiy, 1989). Subsequent exposure of these rocks, coupled with drift into their present positions, has led to a latitudinally symmetrical distribution of sandstone exposure with a maximum at low latitude. In general, there is considerable latitudinal variation in relative exposure area that, together with equator-to-pole climate trends, could enhance or diminish global weathering rates. This variation, and the ties to climate, would be masked by taking global averages.

The high proportion of sandstone exposure for the Recent map (45 percent of non-shield exposures; table 3) was somewhat unexpected. Earlier estimates, based on *volume* percentages (Meybeck, 1987), were much lower (21 percent). This difference is largely compensated for by shale exposures, which represent 25 percent of all non-shield exposures in our map, but 45 percent in Meybeck's estimate.

One contributor to this discrepancy arises from a problem of nonspecificity of rock designation in Ronov's earlier maps. Terrestrial clastics

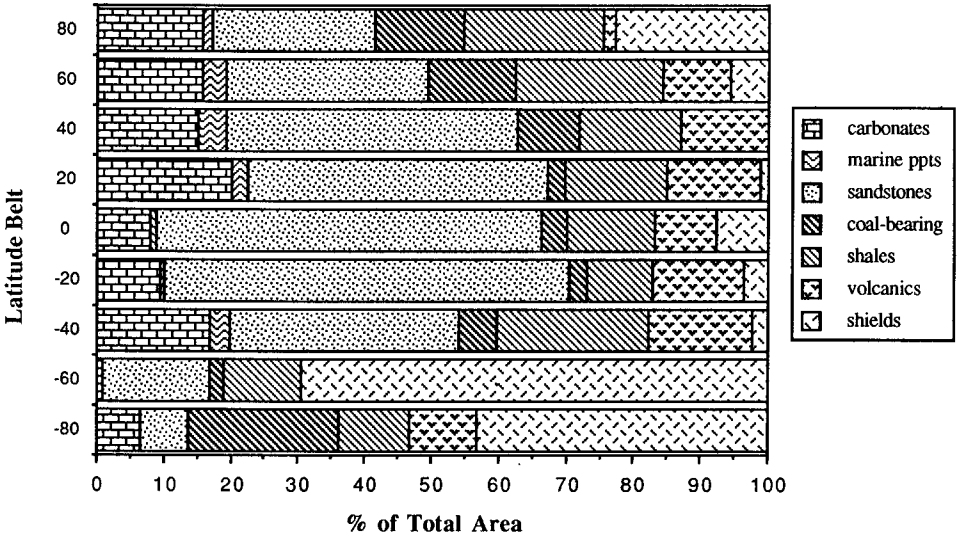

Fig. 5. Latitudinal distribution of rock exposed. Latitude belts 20 degrees centered about given values. Marine precipitates include evaporite and chert.

rocks were undifferentiated in terms of grain size, so we considered them all to be sandstone. However, a check against the new maps of Ronov, Khain, and Balukhovskiy (1989) suggests this contribution is non-negligible, but small.

Another, more interesting possibility is that sandstone is indeed "over-represented" in exposure area, relative to its reservoir volume or mass, due to a characteristic geometry of sandstone deposits: one that is laterally extensive, but thin. This geometry would be characteristic of basin-margin deposits or transgressive sheets and would be in contrast to a more-nearly equant shape for deposits located in the center of basins,

TABLE 2

Recent distribution of rock exposures over 20 degree latitude belts

Latitude	total area	carbonate	marine ppt	sandstone	coal-shale	shale	volcanic	shield
90N-70N	4.0	0.6	0.0	1.0	0.5	0.8	0.1	0.9
70N-50N	28.0	4.4	1.0	8.5	3.6	6.1	2.9	1.5
50N-30N	31.6	4.8	1.4	13.4	2.9	4.7	4.1	0.0
30N-10N	26.4	5.3	0.7	14.1	0.9	4.8	4.4	0.4
10N-10S	20.6	1.6	0.3	18.1	1.2	4.1	2.9	2.4
10S-30S	18.8	1.8	0.1	11.3	0.5	1.8	2.5	0.7
30S-50S	5.1	0.9	0.1	1.7	0.3	1.1	0.8	0.1
50S-70S	1.9	0.0	0.0	0.3	0.0	0.2	0.0	1.3
70S-90S	11.2	0.7	0.0	0.8	2.5	1.2	1.1	4.8

*Data are given in 10^6 km^2. Marine ppt = siliceous + evaporite, volcanic = basalt + rhyolite + andesite.

TABLE 3

Relative proportions of exposure areas*

Rock Type	This Work	Meybeck (1987)**
plutonic and metamorphic	8***	26†
volcanic	12	8
sandstone	41	16
shale	23‡	33
carbonate	14†††	16
evaporites	2	1

*expressed in percentage of total
**based on volume percentages
***shield designation
†based on estimate of Blatt and Jones (1975)
‡includes coal-bearing shales
†††includes siliceous rocks

where shales would tend to accumulate. A careful compilation of depositional area/thickness data must be carried out to test this idea.

The underrepresentation of shield areas in the geologic map (fig. 4A) has been discussed; recall that it arises because of Ronov's attempt to reconstruct original depositional areas. The procedure outlined here for construction of paleogeologic maps is incapable of stripping away these sediments, because the timing of the erosional events is not known. Thus, in our procedure once sediment or volcanic rock is deposited it remains for all time and will be the exposed rock type for all subsequent times unless it is "buried" by a younger depositional unit.

GEOLOGIC TRENDS OVER THE PHANEROZOIC

To investigate Phanerozoic trends in rock exposure, we have created paleogeologic maps for each Period (in fact, for almost every Epoch) of the Phanerozoic. The resulting maps have not been rotated into their paleogeographic positions; only global trends can be considered.

The apparent Phanerozoic trends in relative exposure area, for sedimentary and volcanic rock (fig. 6A), are mostly monotonic. Sandstone exposure increases in proportion, while volcanic and shale exposure decreases. Marine precipitates (cherts and evaporites) maintain a low proportion of the total exposure area throughout the Phanerozoic. The relative area of carbonate exposure increases through the early Paleozoic, peaks in the Devonian, and then decreases through the rest of Phanerozoic time. Coal-bearing shale exposure first appears in the Carboniferous, increases rapidly, and reaches a steady proportion for the Mesozoic and Cenozoic. The increase in coal-bearing shale exposure occurs at the expense of other shale exposures, so considered together, shale maintains a fairly constant exposure proportion through the Phanerozoic.

A striking feature of these trends is their subdued temporal variability. This is especially apparent when one compares exposure area to depositional area trends (fig. 6B); changes in the depositional proportions of the various rock types have been significantly more episodic

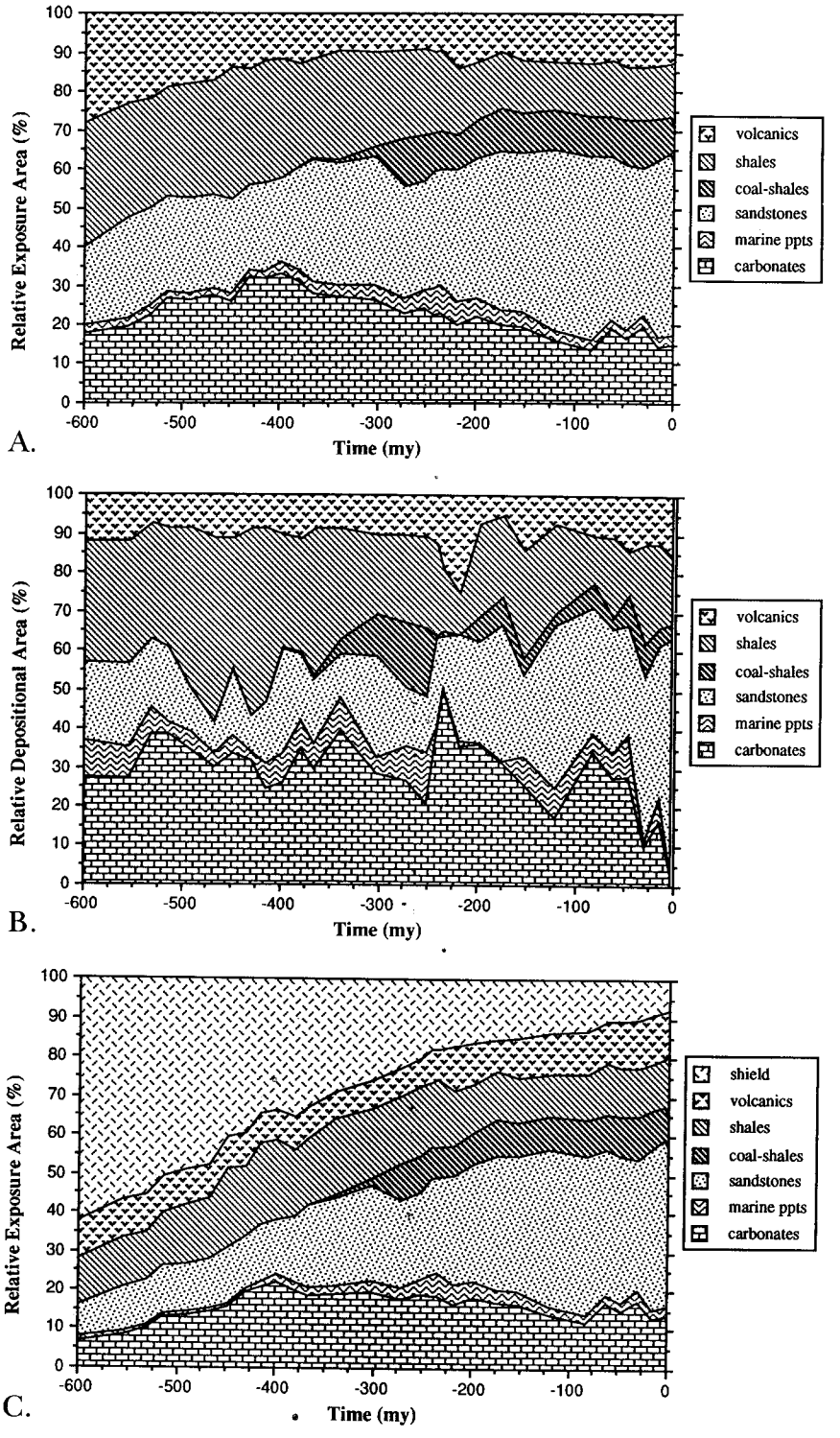

Fig. 6. Area of rock types as a fraction of the total area of (A) exposure, and (B) deposition of volcanic and sedimentary rock, and of (C) all rock, for Epochs of the Phanerozoic.

through time. For instance, carbonate deposition experienced four major peaks during the Phanerozoic (fig. 6B), but none of these is readily apparent in the exposure trend (fig. 6A), even if one allows for a time lag between deposition and exposure.

The damped variation in the relative proportions of exposed rock types reflects the fact that rocks exposed to weathering at any instant are the cumulative results of all past deposition and erosional events. For most time periods, the excursions in depositional area are small relative to the total area of exposure and so do little to modify relative proportions of exposure. The "momentum" of such a feature is also implicit in past geochemical cycling models (BLAG), where exposure area of a given rock type is assumed proportional to its sedimentary mass (a slowly-changing value indeed).

If the shield exposures are considered along with their sedimentary and volcanic counterparts (fig. 6C), a new feature appears as the dominant Phanerozoic trend: a substantial decrease in the relative exposure area of shield rock, coupled to an essentially compensatory increase in sandstone. As discussed before, sandstone exposure for the Recent, and indeed for the entire Cenozoic, has been dominated by rock exposed on Africa, Eurasia, and South America. According to Ronov's maps, there was little deposition on the interiors of Africa and South America during the Paleozoic. Our Paleozoic maps, then, display these continents with shield (pre-Riphean) exposure. As deposition (mainly of sandstone) intensified on these continents through the Mesozoic and Cenozoic, the shield exposures were replaced by sedimentary ones. Because our method is incapable of subsequently "eroding" sediment, the shields remain covered for the rest of the Phanerozoic.

An alternative interpretation of the trend of decreasing shield exposure through time is that it is entirely artificial; shield rock (crystalline basement) has a higher probability of preservation than other rock types (Veizer and Jansen, 1979) and thus will tend to be overrepresented on maps of early time periods. In this sense, the relative area of "shield" exposure is simply a reflection of uncertainty and of the nature of the preserved record. This problem is somewhat obviated by Ronov's attempt to reconstruct original areas of deposition from an increasingly scanty record of older times. Nevertheless, given our technique's inability to specify times or intensities of erosion, this interpretation is certainly viable; our confidence in the maps is greater for younger time periods.

A comparison of the actual areas of Phanerozoic erosion and deposition reveals some intriguing patterns (fig. 7; table 4). For all the trends, changes in land area must be factored in: high sealevel provides increased depositional and decreased erosional area for essentially all rock types.

For certain rock types, the erosional area always exceeds the depositional area. This is true for volcanic rocks (fig. 7A), sandstones (fig. 7B), and coal-bearing shales (fig. 7C). These types typically are deposited in shallow-water or subaerial settings that are less likely to be reflooded,

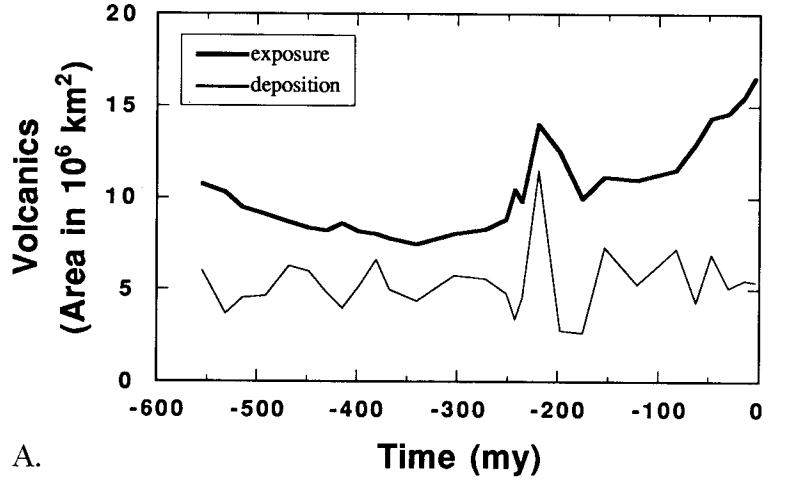

A.

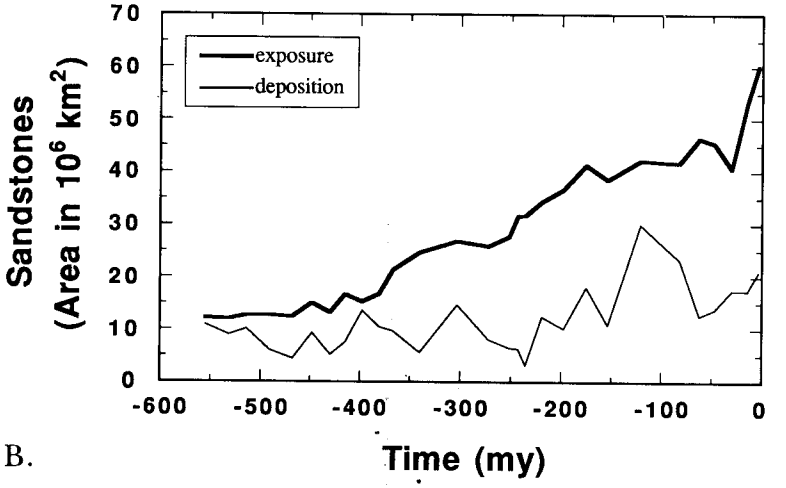

B.

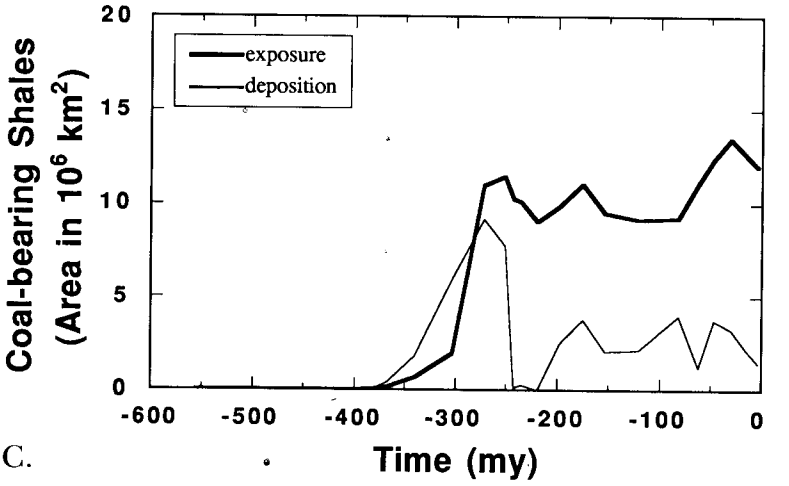

C.

Fig. 7. Depositional and exposure areas of rock types for Epochs of the Phanerozoic. (A) Volcanic rock, (B) Sandstone, (C) Coal-bearing shale.

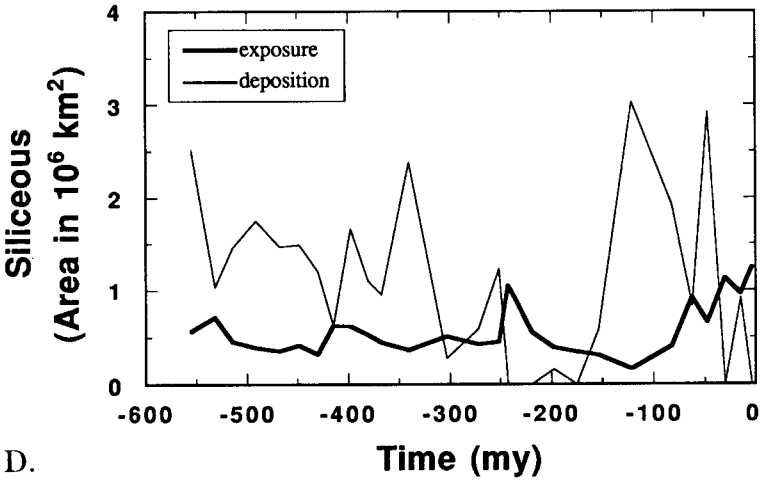

D.

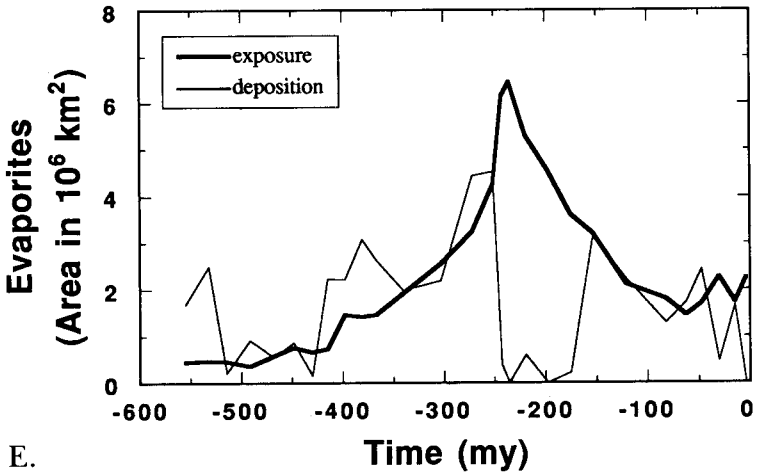

E.

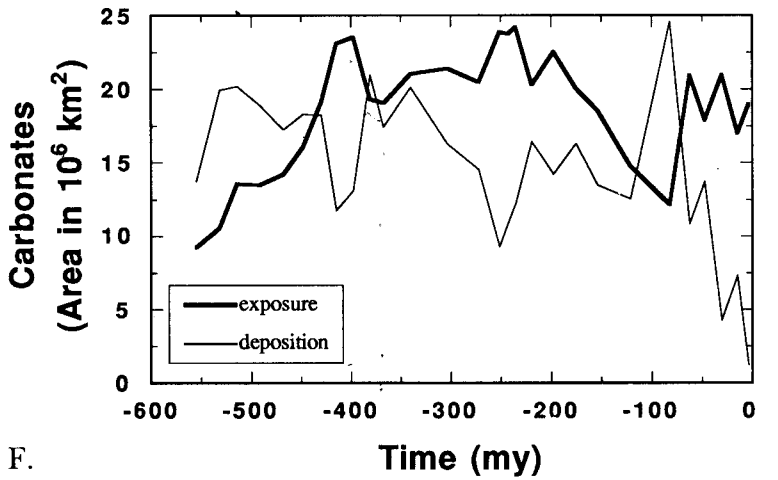

F.

Fig. 7 (continued) (D) Chert (siliceous rock), (E) Evaporite, (F) Carbonate.

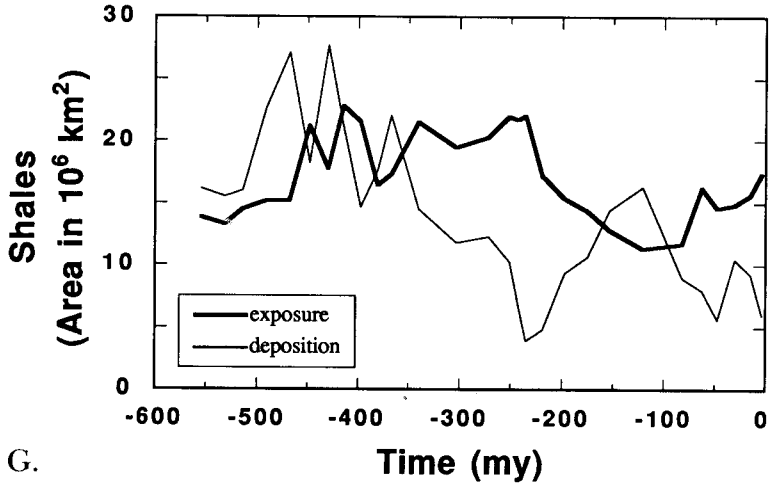

(G) Shale.

Thus, because our technique only removes erosional areas by subsequent deposition, rocks deposited in inland settings tend to accumulate global exposure area. This is an artifact, one that does not reflect the high susceptibility to erosion such deposits experience.

Siliceous rocks (fig. 7D) provide a nice contrast to volcanics, sandstones, and coal-bearing shales. Their depositional area is nearly always in excess of their erosional area, reflecting a deeper-water depositional locus. Such a site is likely to both remain flooded and experience subsequent deposition of other rock types.

Evaporite (fig 7E), limestone (fig. 7F), and shale (fig. 7G) deposition and exposure follow one another quite closely. The two processes could be said to be in "steady state" for these rock types, in the sense that general exposure trends parallel depositional trends. For evaporites this is particularly true; they are exposed soon after deposition and are thereafter soon buried by other rock types unless deposition resumes. Their peak of exposure follows a period of steadily increasing deposition through the Paleozoic, the maximum of which was directly followed by a large increase in land area. The presumed sealevel fall exposed a large amount of evaporites to dissolution. For limestones and shales, exposure exceeded depositional area during long-term lowstands of global sealevel (late Paleozoic to early Mesozoic and Cenozoic) and vice-versa during highstands.

SUMMARY

1. A simple method of paleogeologic reconstruction has been devised using lithofacies data. The primary database has been the series of maps published by A.B. Ronov and his coworkers over the past several decades.

TABLE 4

Exposed land area of rock units: Paleogeologic results for the Phanerozoic

Period	Carbonate	Sandstone	Siliceous	Volcanic	Evaporite	Shield	Shale	Coal	Total
Recent	20.1	60.9	1.2	17.0	2.2	11.4	22.6	12.0	147.5
Pliocene	19.0	60.2	1.2	16.6	2.2	11.4	17.3	12.0	139.9
Miocene	17.0	53.3	1.0	15.5	1.7	11.6	15.6	12.6	128.3
Oligocene	21.0	40.6	1.1	14.6	2.3	12.4	14.8	13.5	120.3
Eocene	18.0	45.5	0.7	14.4	1.7	12.6	14.6	12.4	119.7
Paleocene	21.0	46.4	0.9	13.0	1.4	13.0	16.2	11.1	122.9
L Cretaceous	12.2	41.7	0.4	11.5	1.8	13.4	11.7	9.2	101.8
E Cretaceous	14.8	42.2	0.2	11.0	2.1	14.3	11.3	9.2	104.9
L Jurassic	18.5	38.5	0.3	11.1	3.2	16.4	12.8	9.5	110.3
M Jurassic	20.1	41.2	0.3	10.0	3.6	17.9	14.3	11.1	118.5
E Jurassic	22.5	36.7	0.4	12.5	4.5	19.9	15.4	9.9	121.8
L Triassic	20.3	34.3	0.6	14.0	5.3	20.7	17.2	9.0	121.3
M Triassic	24.2	31.7	0.9	9.8	6.4	23.1	22.0	10.1	128.3
E Triassic	23.7	31.6	1.0	10.4	6.1	23.2	21.7	10.2	128.1
L Permian	23.9	27.7	0.4	8.8	4.2	24.9	21.9	11.5	123.3
E Permian	20.5	25.8	0.4	8.3	3.2	26.0	20.3	11.0	115.4
ML Carboniferous	21.4	26.7	0.5	8.0	2.5	28.2	19.5	1.9	108.9
E Carboniferous	21.0	24.6	0.4	7.4	1.9	31.6	21.5	0.7	109.1
L Devonian	19.1	21.3	0.4	7.8	1.5	33.2	17.3	0.2	100.6
M Devonian	19.3	16.7	0.5	8.0	1.4	34.3	16.4	0.1	96.7
E Devonian	23.5	15.2	0.6	8.1	1.4	35.9	21.5	0	106.3
L Silurian	23.1	16.6	0.6	8.6	0.7	38.1	22.8	0	110.5
E Silurian	19.1	13.1	0.3	8.2	0.7	38.6	17.8	0	97.80
L Ordovician	16.1	15.0	0.4	8.3	0.8	41.7	21.2	0	103.4
M Ordovician	14.2	12.3	0.4	8.6	0.6	46.4	15.2	0	97.7
E Ordovician	13.5	12.6	0.4	9.1	0.4	48.8	15.1	0	99.8
L Cambrian	13.6	12.6	0.5	9.5	0.5	52.3	14.5	0	103.3
M Cambrian	10.6	11.9	0.7	10.3	0.5	58.2	13.3	0	105.4
E Cambrian	9.2	12.1	0.6	10.7	0.5	61.3	13.8	0	108.2

*Data are given in 10^6 km^2. Abbreviations: L = Late, M = Middle, E = Early.

2. The sedimentary contribution to the inferred Recent geology shows an age distribution similar to that of present-day exposures. Both the observed rock record and our results show distinct departures between Devonian and Jurassic times from a strictly log-normal relationship, which coincide with the initiation and termination of supercontinental, tectonic stasis and thus lowered, global erosion rates.

3. The constructed geologic map for the Recent reproduces much of the present-day exposures of igneous rocks and marine and continental clastics. Some discrepancies, such as in the size of continental shield areas, cannot be fully resolved, because the timing of their exposure is not accurately known.

4. The results of the paleogeologic reconstructions exhibit two major Phanerozoic features. First, large temporal variations in relative areal extents of volcanic and sedimentary deposits are not reflected in the more subdued record of variation in the areal extents of exposed rock types. Second, the extent of sandstone exposure determined by this method has increased through the Phanerozoic, largely at the expense of a decrease in shield exposure.

5. Model weathering relations that assume first-order dependence on reservoir mass do indeed capture the damped nature of temporal variability in relative global exposure areas of rock types. However, they cannot address the interesting question of if, by a combination of sedimentation history and continental drift, changes in climate and exposure distributions might have conspired to affect significantly global weathering and CO_2 consumption rates. The determination of paleogeologic distributions should ultimately provide a great advantage over parameterizations based on global estimates of sedimentary reservoirs.

ACKNOWLEDGMENTS

This work was funded by a grant from the National Science Foundation (EAR-8720551) to the Earth System Science Center at The Pennsylvania State University. "Additional support to G.J.S.B. has been contributed by NASA Goddard Space Flight Center and the Universities Space Research Association." Computer programming assistance was provided by W. Peterson. This manuscript was considerably improved by comments from E. Barron, R. Berner, and A. Rose, and by an especially helpful and thought-provoking review by B. Wilkinson.

REFERENCES

Berner, R. A., 1990, Atmospheric carbon dioxide levels over Phanerozoic time: Science, v. 249, p. 1382–1386.

Berner, R. A., Lasaga, A. C., and Garrels, R. M., 1983, The carbonate-silicate geochemical cycle and its effect on atmospheric carbon dioxide over the past 100 million years: American Journal of Science, v. 283, p. 641–683.

Blatt, H., and Jones, R. L., 1975, Proportions of exposed igneous, metamorphic, and sedimentary rocks: Geological Society of America Bulletin, v. 86, p. 1085–1088.

Choubert, G., and Faure-Muret, A., eds., 1981, Atlas geologique du monde: Comission de la Carte Geologique du Monde, Bureau de Cartographic Geologique Internationale, UNESCO, Paris, 22 sheets.

Cook, T. D., and Bally, A. W., editors, 1975, Stratigraphic atlas of North and Central America: Princeton, N.J., Princeton University Press, 272p.

Derry, D. R., 1980, World Atlas of Geology and Mineral Deposits: New York, John Wiley & Sons, 110 p.
Garrels, R. M., and Mackenzie, F. T., 1971, Gregor's denudation of the continents: Nature, v. 231, p. 382–383.
Gregor, C. B., 1968, The rate of denudation in post-Algokian time: Royal Netherlands Academy of Science Proceedings, v. 71, p. 22–30.
———— 1985, The mass-age distribution of Phanerozoic sediments, *in* Snelling, N. J., ed., The Chronology of the Geologic Record (published for The Geological Society): Oxford, Blackwell Scientific Publications, p. 284–288.
Herak, M., and Stringfield, V. T., 1972, Karst—Important Karst Regions of the Northern Hemisphere: Amsterdam, Elsevier, 551 p.
Khain, V. Ye., Ronov, A. B., and Balukhovskiy, A. N., 1975, Cretaceous lithologic associations of the world: Sovetskaya Geologiya, no. 11, p. 10–39 (translated in International Geology Review, 1976, v. 18, p. 1269–1295).
———— 1979, Neogene lithologic associations of the continents: Sovetskaya Geologiya, no. 10, p. 3–35 (translated in International Geology Review, 1981, v. 23, p. 426–454).
Kutzbach, J. E., and Gallimore, R. G., 1989, Pangaean climates: Megamonsoons of the megacontinent: Journal of Geophysical Research, v. 94, p. 3341–3357.
Lasaga, A. C., Berner, R. A. and Garrels, R. M., 1985, An improved geochemical model of atmospheric CO_2 over the past 100 million years, *in* Sundquist, E. T., and Broecker, W. S., editors, The Carbon Cycle and Atmospheric CO_2: Natural Variations Archean to Present: Washington, D.C., American Geophysical Union, p. 397–411.
Levorsen, A. I., 1960, Paleogeologic Maps: San Francisco, W. H. Freeman and Co., 174 p.
Mackenzie, F. T., and Pigott, J. D., 1981, Tectonic controls of Phanerozoic sedimentary rock cycling: Journal of the Geological Society of London, v. 138, p. 183–196.
Meybeck, M., 1987, Global chemical weathering of surficial rocks estimated from river dissolved loads: American Journal of Science, v. 287, p. 401–428.
Ronov, A. B., and Khain, V. Ye., 1961, Triassic lithologic associations of the world: Sovetskaya Geologiya, no. 1, p. 27–48.
———— 1962, Jurassic lithologic associations of the world: Sovetskaya Geologiya, no. 1, p. 9–34.
Ronov, A. B., Khain, V. Ye., and Balukhovskiy, A. N., 1978, Paleogene lithologic associations of the continents: Sovetskaya Geologiya, no. 3, p. 10–42 (translated in International Geology Review, 1979, v. 21, p. 415–446).
———— 1983, Late Mesozoic and Cenozoic lithologic associations of the continents and oceans: Sovetskaya Geologiya, no. 6, p. 32–45.
———— 1989, Atlas of Lithological-Paleogeographical Maps of the World. Mesozoic and Cenozoic of continents and oceans: Leningrad, Nauka, 79 p.
Ronov, A. B., Khain, V. E., Balukhovsky, A. N., and Seslavinsky, K. B., 1980, Quantitative analysis of Phanerozoic sedimentation: Sedimentary Geology, v. 23, p. 311–325.
Ronov, A. B., Khain, V. Ye., and Seslavinskiy, K., 1984, Atlas of Lithological-Paleogeographical maps of the World. Late Precambrian and Paleozoic of continents: Leningrad, Nauka, 70 p.
Snead, R. E., 1980, World Atlas of Geomorphic Features: New York, Kreiger Publishing Company, Inc., 301 p.
Veizer, J. and Jansen, S. L., 1979, Basement and sedimentary recycling and continental evolution: Journal of Geology, v. 87, p. 341–370.
Worsley, T. R., Nance, R. D., and Moody, J. B., 1986, Tectonic cycles and the history of the Earth's biogeochemical and paleoceanographic record: Paleoceanography, v. 1, p. 233–264.